

Methanation Pilot Plant with a Slurry Bubble Column Reactor: Setup and First Experimental Results

Simon Sauerschell,* Siegfried Bajohr, and Thomas Kolb

Cite This: *Energy Fuels* 2022, 36, 7166–7176

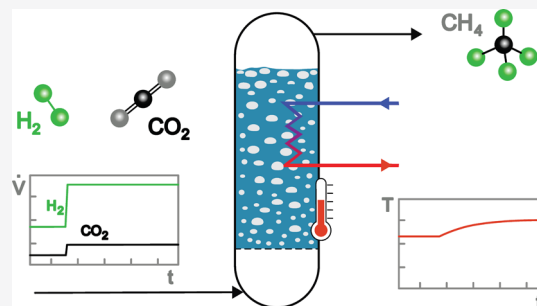
Read Online

ACCESS |

Metrics & More

Article Recommendations

ABSTRACT: As a part of various research projects, a methanation pilot plant with a slurry bubble column reactor (SBCR) was commissioned and operated. The plant has a nominal load of a 100 kW methane output (lower calorific value) with a reactor diameter of 260 mm and a reactor length of 2500 mm. First experimental data on the steady-state and dynamic operation of catalytic CO₂ methanation are presented. Steady-state results from laboratory-scale studies (<1 kW methane output) published previously were confirmed qualitatively at the pilot plant eliminating wall effects unavoidable in small-scale reactors. As predicted, high H₂/CO₂ ratios increase CO₂ conversion, but excess H₂ apparently promotes decomposition of the liquid phase (dibenzyltoluene) used in the bubble column reactor. Additionally, due to the increased reactor dimensions compared to laboratory equipment, it was now possible to observe a thermal response of the SBCR under conditions of rapid gas load changes characteristic of envisaged power-to-gas applications with volatile renewable electricity. As the predicted robustness of the SBCR-concept toward a dynamic operation with fast load changes was demonstrated successfully, it offers an attractive alternative to the established fixed-bed methanation technologies with their inherent limitations on dynamic operability.



INTRODUCTION

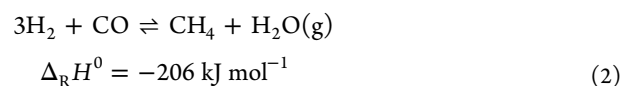
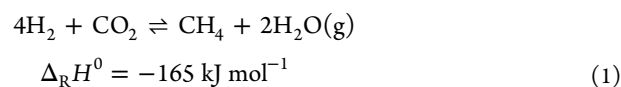
To this date, a total of 193 countries are parties to the Paris Agreement from 2016¹ and thus signed up to keep the increase in the global average temperature considerably below 2 K. In order to live up to this agreement, fossil energy sources have to be replaced by renewable energies. Owing to the unavoidable fluctuating availability of solar- and wind-based power production, energy storage concepts are crucial for a successful implementation of a stable and reliable future energy system.²

A promising way of storing renewable energies is the power-to-gas-process. Therein, as a first step, hydrogen (H₂) is produced via water electrolysis and can be used directly as a chemical energy carrier if the necessary infrastructures and applications are at hand. At the moment, a nationwide H₂ infrastructure is not available in Germany, and it has to be established in the next decades to facilitate such concepts. Furthermore, there are many applications (e.g., all products from organic chemistry) that require carbon in conjunction with H₂ and which cannot be served by pure H₂. Therefore, the conversion of regenerative H₂ with a suitable carbon source such as carbon dioxide (CO₂) via catalytic methanation to the established chemical energy carrier methane (CH₄) is an attractive alternative for decarbonization. CH₄ offers the benefit of an excellent storage, distribution, and utilization infrastructure based on the omnipresent natural gas grid.^{3,4} Furthermore, recent developments focus on the increase of liquefied natural gas as fuel for mobile applications, which is

also an attractive utilization path for synthetic methane with a low carbon footprint.⁵

Suitable carbon sources for catalytic methanation are carbon monoxide (CO) or CO₂. A supply of nonfossil CO and CO₂ for future power-to-gas applications may stem from biomass gasification.⁶ Alternatively, CO₂ may be captured from industrial exhaust gases⁷ or ambient air.⁸ However, it has to be mentioned that CO₂ from industrial exhaust gases often originates from fossil resources (e.g., cement production or coal-fired power plants).

Both methanation reactions



Received: March 7, 2022

Revised: May 19, 2022

Published: June 8, 2022



are exothermic and volume-reducing. Therefore, low temperatures and high pressures are preferable to shift the equilibrium composition toward methane. However, in order to achieve adequate reaction rates, temperatures well above 200 °C and the application of catalysts are necessary for technical processes, while pressures typically range from approx. 5 to 100 bar.⁹

While methanation is receiving a growing attention in the context of power-to-gas process chains, its original and probably still most common industrial application is the removal of CO traces from H₂-rich feed gases in ammonia plants.^{10–12} Over decades, the only large-scale catalytic methanation, with methane being the target product, was the Great Plains Synfuels Plant (Beulah, USA), which was the first commercial coal-to-SNG (synthetic natural gas) plant. It started operation in 1984 and has a production capacity of 1500 MW of SNG.¹³ However, within the past 10 years various coal-to-SNG plants have been built in China/Inner Mongolia.^{14,15} Furthermore, in 2014, the GoBiGas demonstration plant was commissioned for investigation of a biomass-to-SNG concept at a scale of 20 MW.⁶

As shown above, the coal-to-SNG concept has been economically feasible for a long time. Renewable methane from power-to-gas, on the other hand, is still too costly to compete with natural gas.¹⁶ Nevertheless, in the past few years, several demonstration-scale plants have been built. The largest power-to-gas plant to this date is the Audi e-gas plant in Werlte (Germany),^{16,17} with a single fixed-bed methanation reactor and a maximum output of roughly 3.5 MW of SNG.¹⁸ Other examples are a honeycomb methanation plant (approx. 600 kW SNG output) in Falkenhagen (Germany),^{3,4,19} a biological stirred bubble column methanation (approx. 350 kW) in Solothurn (Switzerland),^{3,19} and a methanation plant with a microstructured reactor (approx. 100 kW) in Troia (Italy),^{3,19} all built within the research project STORE&GO.

Regarding the reactor concepts developed and employed up to now, various fixed-bed and fluidized-bed concepts for SNG production have been investigated in the 1970s, while more recent investigations also focus on structured reactors (honeycomb- and microreactors)^{4,20–24} and three-phase reactors.^{25–28}

A main advantage of three-phase reactors is their high robustness during dynamic operation because the liquid phase removes the reaction heat very efficiently from the catalyst surface and buffers load changes due to its inherently high heat capacity. This makes three-phase reactors a promising reactor technology for power-to-gas applications. Drawbacks are, however, the additional mass transfer resistance from gas phase to catalyst due to the intermediary liquid phase and unwanted reactions of the liquid phase with reactants and/or the catalyst. Furthermore, catalyst activation within a three-phase system is often difficult due to thermal limitations of the liquid phase and the required conditions for the activation process.

The first research on three-phase CO-methanation in slurry bubble column reactors (SBCRs) was reported by Hammer²⁹ in the 1960s. Commercialization was not intended, and methanation was merely used as a model reaction to study the interactions between reaction kinetics, mass transport, and hydrodynamic phenomena in SBCRs. First attempts toward the commercialization of three-phase methanation were made in the 1970s by the company Chem Systems Inc., which patented a concept for CO methanation in a three-phase-

fluidized-bed reactor.³⁰ A pilot plant with a reactor of approx. 600 mm diameter and 4600 mm height³¹ was set up and commissioned at the IGT HYGAS in Chicago, Illinois.³² By 1978, a time-on-stream of 2347 h from a total of 7 test runs was reported with 122 h of methanation with HYGAS synthesis gas and 193 h with steam-methane reformer gas. During the test runs, a CO conversion of up to 100% was observed.³³ Besides these developments, the authors did not find any reports regarding further scaleup from the pilot to commercial scale.

In contrast to the three-phase fluidized bed from Chem Systems Inc., more recent studies on three-phase methanation focus again on SBCRs. Götz et al.^{34,35} investigated the suitability of different ionic liquids and heat transfer oils for application as a liquid phase in three-phase methanation. The ionic liquids showed a strongly reduced thermal stability under a H₂ atmosphere. Amongst all the liquids studied, dibenzyltoluene (DBT), often used as heat transfer oil, was eventually identified as the most suitable liquid phase for three-phase methanation.^{36,37} In a further publication by Götz et al.,³⁸ experimental results on the hydrodynamics of various liquids were presented. Lefebvre et al.²⁵ carried out experimental studies to identify optimal process conditions for CO₂ methanation in a laboratory-scale SBCR. They found high pressures, temperatures, and H₂/CO₂ ratios to increase the reactor performance. Also, experimental studies were conducted on the reaction kinetics of three-phase CO₂ methanation in a continuous stirred tank reactor²⁶ and were compared to the reaction kinetics of two-phase CO₂ methanation.²⁷ It was found that the liquid phase does not have an influence on the microkinetics and experimental results from three-phase methanation can be described fairly well by a two-phase kinetic rate equation. However, the liquid phase influences macrokinetics due to the changed reactant concentrations at the catalyst surface depending on the solubility of the reactant gases. A modeling approach toward a steady-state and transient operation of two- and three-phase CO₂-methanation was presented in ref 28. Simulations for the transient operation showed small temperature changes in the three-phase reactor during dynamic load changes, whereas the two-phase methanation reactor (tube bundle reactor) exhibited an unacceptably high-temperature increase in the hot spot.

Research on new catalysts for three-phase CO methanation was presented by Zhang et al.³⁹ and Meng et al.^{40,41} The authors developed different Ni/Al₂O₃-catalysts for slurry reactor methanation and tested them in lab-scale continuously stirred tank reactors using a liquid paraffin mixture as the slurry solvent.

Since the mass transfer rate can be the limiting step for three-phase methanation,²⁵ hydrodynamics is an important issue in SBCR methanation. It has been stated by various authors^{42–44} that gas holdup, which is considered an important hydrodynamic parameter in bubble columns, does not depend on the reactor diameter if the latter exceeds approximately 0.15 m. This observation is mostly attributed to wall effects, which become considerably weaker at larger diameters. Slim bubble column reactors are also prone to slug flow, a flow regime that can occur at high superficial gas velocities and which is generally considered to be undesired and without any technical relevance in industrial bubble columns. Depending on the system properties and reactor height, the slug flow can even be observed for maximum reactor diameters of 0.20 m.⁴⁵



Figure 1. Photo of the SBCR methanation pilot plant at the KIT Energy Lab 2.0 (reprinted with permission from ref 48).

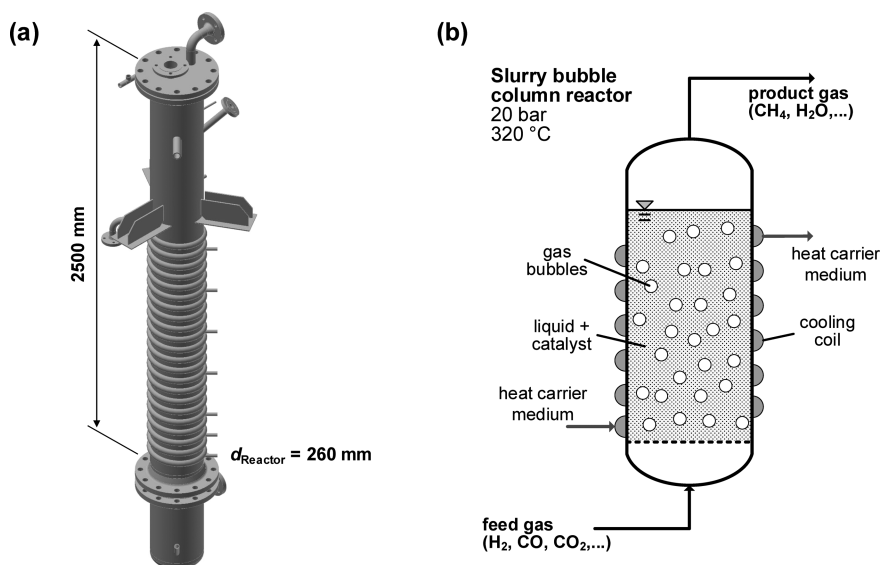


Figure 2. 3D drawing of the SBCR of the Energy Lab 2.0 methanation plant (a) and schematic drawing of the SBCR (b).

Thus, experimental data from reactors with larger diameters are of importance as basis for a reliable scale-up model. Additionally, more hydrodynamic data for different fluids and process conditions, which are relevant in industry (e.g., hydrocarbons and elevated temperatures and pressures) are desirable. However, to carry out experiments under such conditions, high efforts regarding costs and safety aspects have to be made, and therefore, such data is rare in the literature.⁴⁶

PILOT PLANT DESCRIPTION

The methanation pilot plant presented in this paper (photo: see Figure 1) was built as part of the research infrastructure “Energy Lab 2.0” at the Karlsruhe Institute of Technology (KIT) in 2018/2019. The Energy Lab 2.0 is a large research facility for renewable energy systems. As a real-life laboratory and simulation platform, it enables the partner institutions KIT, Forschungszentrum Jülich (FZJ), and German Aerospace Center (DLR) to investigate the interplay of components in the smart, connected energy systems of the future.⁴⁷

Slurry Bubble Column Reactor. The SBCR methanation is operated at a maximum pressure and temperature of 20 bar and 330 °C, respectively, and has a methane output of up to 10 m³/h (STP), which is equivalent to an enthalpy flow of approximately 100 kW. A 3D drawing of the bubble column reactor is shown in Figure 2a. It has an inner diameter of 260 mm and a useable height of 2200 mm above the gas sparger. A cooling coil is welded onto the outer surface of the reactor to remove the reaction heat by means of a circulating heat carrier medium.

The functional principle of the SBCR is displayed in Figure 2b. The reactant gas mixture is fed into the reactor at the bottom. Above the gas sparger, the reactor is filled with a suspension fluid (=slurry) consisting of an inert liquid phase and a solid catalyst in the form of fine particles (diameter < 100 μm). The bubbles evolving at the gas sparger rise through the slurry toward the top of the reactor. During that process, the reactants dissolve in the liquid phase and react at the catalyst surface according to eqs 1 and 2. The products CH₄ and H₂O are transported from the catalyst back into the gas

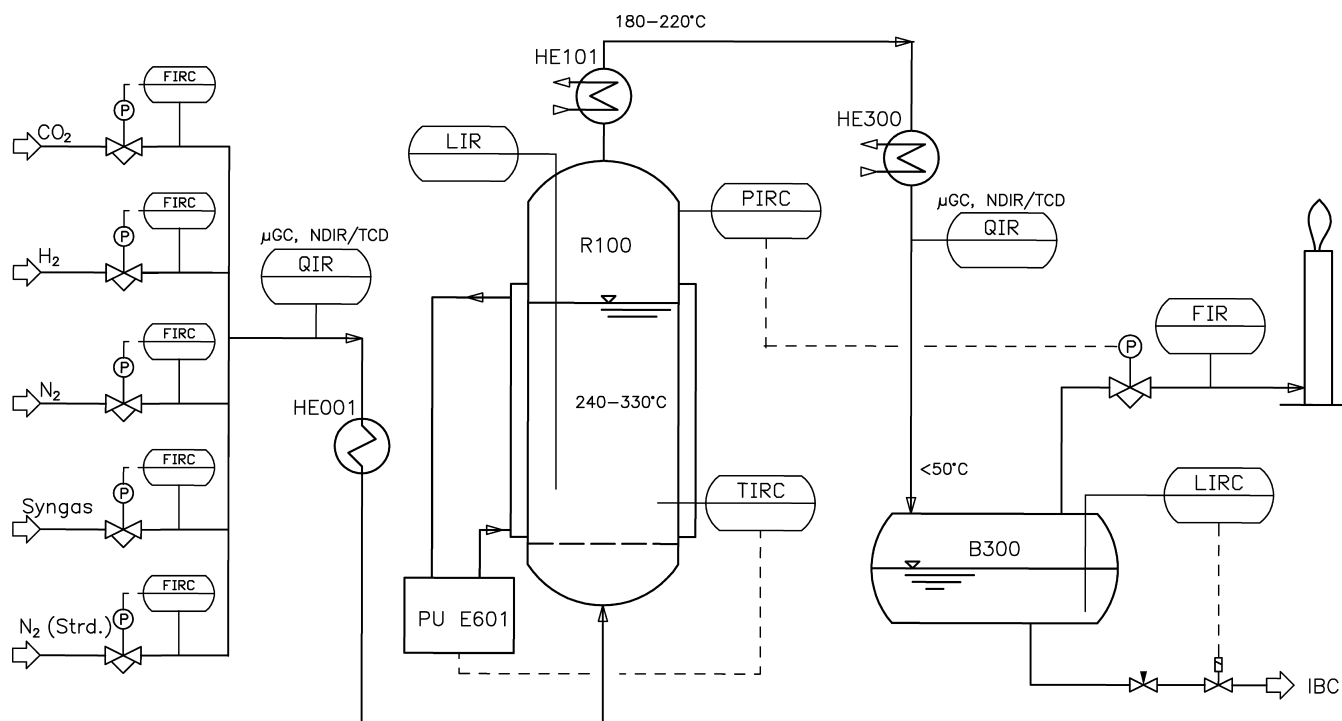


Figure 3. Simplified P&ID of the methanation pilot plant.

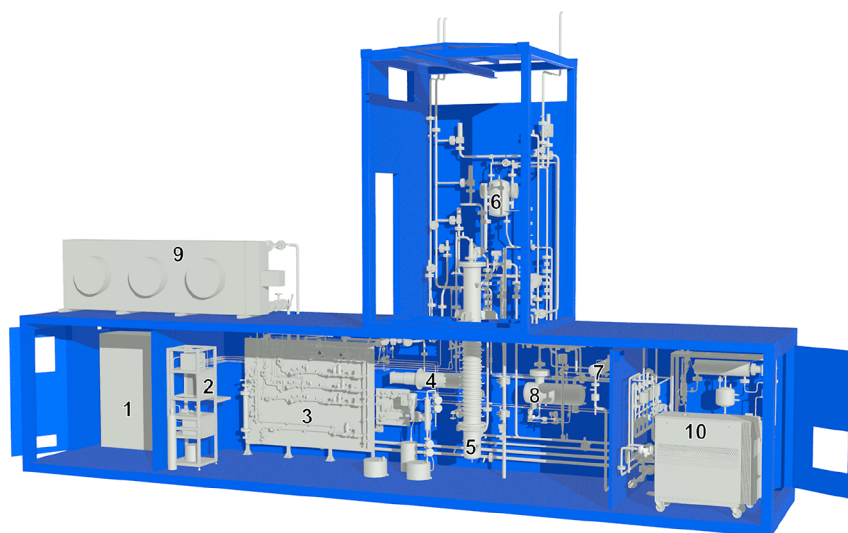


Figure 4. 3D drawing of the Energy Lab 2.0 methanation pilot plant (by FRINTEC GmbH, Frankfurt, Germany). (1) Control cabinet, (2) analytics, (3) gas dosing, (4) electric preheater HE001, (5) SBCR R100, (6) heat exchanger HE101, (7) heat exchanger HE300, (8) condensate tank B300, (9) ambient air cooler, and (10): temperature control unit PU E601.

phase, that is, the product gas concentration increases, and the reactant gas concentration decreases in the gas phase on its way upward. Finally, the product gas stream leaving the reactor at the top is analyzed and flared before releasing to the ambient.

Process Description. A simplified P&I diagram of the methanation plant is shown in Figure 3. Reactant gases are fed to the system by mass-flow controllers. As a carbon source for the methanation reaction, CO₂ is supplied from a storage tank. Alternatively, a CO/CO₂/H₂ syngas from the adjacent bioliq gasification plant⁴⁹ serves as the carbon and hydrogen source. The H₂ necessary for CO₂ methanation is obtained from a buffer tank, which can be fed by a PEM water-electrolysis plant

installed on site. However, for the experiments presented in this paper, bioliq syngas was not used, and the H₂ buffer tank was filled by trailer. Additionally, nitrogen (N₂) is used as a purge gas during the start-up and shut down process and as an internal reference substance for closing mass balances based on the reactant and product gas analysis.

Before entering the reactor, the feed gas is analyzed and heated up to the desired reactor inlet temperature in the electric preheater HE001. Subsequently, it enters the SBCR R100. As mentioned above, in the reactor, the highly exothermic methanation takes place. To remove the reaction heat, the temperature control unit PU E601 circulates a heat

transfer oil (Marlotherm SH) through the cooling coil of the reactor (see also Figure 2).

Especially, at higher temperatures (max. up to 330 °C), the amount of liquid evaporated in the reactor cannot be neglected. To keep losses as low as possible, first, the product gas stream is cooled down to about 200 °C in the heat exchanger HE101, which is constructed in such a way that the condensing liquids directly flow back into the reactor.

In the subsequent condenser HE300, the product gas is finally cooled down to below 50 °C to condense the reaction water. Additionally, the remaining vapors of the liquid phase are condensed together with the water, and the condensate is collected in the tank B300 and discharged automatically into an intermediate bulk container (IBC).

To adjust the pressure in the methanation plant, the product gas leaving B300 is throttled by a control valve. The product gas leaves the plant at nearly ambient pressure. As the plant is operated for research purposes, no further use of the produced methane is intended. Therefore, the gas is flared in an external unit, and the flue gas is emitted to the ambient.

Gas Analytics. The plant is equipped with two gas analyzers (NDIR/TCD, model EL3020 Uras26/Caldos27—TOPGAS manufactured by ABB) and a micro GC (model Fusion 2-Module System manufactured by Inficon). The gas analyzers measure reactant and product gas concentrations (CO, CO₂, CH₄, and H₂) continuously (data is logged every second), while the micro GC alternately takes samples from the reactant and the product gas stream in time intervals of approximately 5 min. The continuous gas analysis is necessary for the evaluation of experiments on dynamic reactor operation, whereas the GC-data is used for the evaluation of stationary experiments, including detailed mass balances.

Plant Setup. The methanation plant is installed in a modified 40 ft shipping container (3D drawing, see Figure 4) within the Energy Lab 2.0 plant network at KIT, Campus North. The process design and commissioning were carried out by Engler-Bunte-Institute, Fuel Technology (EBI ceb) at KIT, while FRINTEC GmbH Frankfurt, Germany, planned and realized the mechanical construction of the plant. The plant works with the commercial process control system PCS7, which was implemented and programmed by Siemens AG Karlsruhe, Germany. Commissioning took place in June 2019.

EXPERIMENTAL PROCEDURE

In this paper, the data from four experimental runs (carried out between October 2019 and August 2020) are presented. During these runs, several experiments under steady-state and transient conditions were performed. Most of the experiments were repeated at least once to check repeatability. The duration of each run was approximately 100 h time-on-stream, with the operating team working in shifts. The runs comprise experiments on CO₂ methanation. CO₂ and H₂ were obtained from the storage tanks mentioned above. The electrolysis plant was shut off during all experiments, and thus, the H₂ tank had to be filled on a daily basis by a trailer.

Materials. The catalyst used was a commercial Ni/SiO₂ catalyst manufactured by BASF SE, Germany, ground to a fine powder (particle size: $x_{50} = 15 \mu\text{m}$, $x_{64} = 60 \mu\text{m}$). Catalyst activation was carried out in a fixed bed reactor on site of the Energy Lab 2.0 according to the manufacturer's instructions under a H₂-atmosphere at about 400 °C and near ambient pressure. The water formed during the activation process was condensed, collected, and its amount was measured as an indication of catalyst activity for the respective run. After finishing the activation procedure, the catalyst was mixed with the liquid phase and transferred to and into the SBCR, avoiding contact with oxygen using a lock hopper system.

The liquid phase used for the experiments was DBT, trade name Marlotherm SH, manufactured by Sasol GmbH, Germany. The relevant properties of Marlotherm SH for this work are shown in Table 1.

Table 1. Properties of DBT (Marlotherm SH)

chemical structure	C ₂₁ H ₂₀ ³⁴
molecular mass <i>M</i>	272 g/mol ³⁴
vapor pressure <i>p</i> _{vap} at 320 °C	0.315 bar ⁵⁰
max. allowed temperature <i>T</i> _{max}	350 °C ⁵⁰
density ρ at 320 °C	830 kg/m ³⁵⁰
Kinematic viscosity ν at 320 °C	0.4 mm ² /s ⁵⁰
Henry's law constant <i>H</i> at 300 °C for H ₂	265 (bar kg)/mol ³⁴
Henry's law constant <i>H</i> at 300 °C for CO ₂	105 (bar kg)/mol ³⁴

Preparation and Startup. For the experiments, approximately 90 kg of DBT and 6.5 kg of activated catalyst were filled into the reactor. After completion of the filling process, the reactor pressure was raised, and the reactor was heated up to the desired start reaction temperature through the outer cooling/heating system. During filling and heating, a constant N₂ flow of 10 m³/h (STP) through the gas sparger was maintained to prevent the liquid from weeping and the catalyst particles from settling. Subsequently, inertization with N₂ was replaced by H₂, and the CO₂ flow was gradually increased, until the desired H₂/CO₂ ratio was achieved. The H₂/CO₂ ratio will be expressed in the following by the stoichiometric number defined by

$$S = \frac{y_{\text{H}_2, \text{in}} \cdot \nu_{\text{CO}_2}}{y_{\text{CO}_2, \text{in}} \cdot \nu_{\text{H}_2}} \quad (3)$$

where $y_{i, \text{in}}$ are the mole fractions of the respective gas species in the feed gas, and ν_i are the stoichiometric coefficients.

Reference Point. In order to be able to assess the comparability of the results, CO₂ conversion at a nominal load (process settings, see Table 2) was measured before and after each series of measurements within an experimental run.

Table 2. Process Settings at a Nominal Load (= Reference Point)

p_{Reactor}	20 bar
T_{Reactor}	320 °C
<i>S</i>	≈1.05
$\dot{V}_{\text{H}_2, \text{in}}$	40 m ³ /h (STP)
$\dot{V}_{\text{N}_2, \text{in}}$	1 m ³ /h (STP)

Steady-State Operation. Several series of measurements at steady-state conditions were carried out with varying reactor temperature, pressure, and stoichiometric number, respectively. The basis for the experiments were the process settings of the reference point, which means that only one of the parameters from Table 2 was varied at a time. For the experiments on the temperature and pressure, this means that the plant was operated at the same input load as the reference point (roughly 95 kW of the methane output at a full CO₂ conversion), while for the experiments on the stoichiometric number, the CO₂ flow and thus load was gradually reduced.

The measurements are similar to the experiments conducted by Lefebvre et al.,²⁵ where the dependence of CO₂ conversion on various parameters was investigated in two lab-scale SBCRs using DBT and a Ni/Al₂O₃ catalyst.

While Lefebvre et al.²⁵ compared results at constant superficial gas velocities u_G , for most of the results presented in this paper, the modified residence time τ_{mod} was kept constant. The parameter τ_{mod} is defined by

$$\tau_{\text{mod}} = \frac{m_{\text{cat}}}{\dot{n}_{\text{CO}_2}} \quad (4)$$

where m_{cat} is the mass of activated catalyst in the reactor, and \dot{n}_{CO_2} is the molar flow of CO_2 in the feed gas.

For evaluation of the experiments, all values measured were averaged for the respective time period of the steady state (usually 60 to 120 min). CO_2 conversion was calculated according to the following equation, using data from the GC analysis of the product gas composition

$$X_{\text{CO}_2} = \frac{y_{\text{CH}_4,\text{out}}}{y_{\text{CO}_2,\text{out}} + y_{\text{CH}_4,\text{out}}} \quad (5)$$

where X_{CO_2} is the CO_2 conversion, and y_i are the mole fractions of the respective gas species. As the mole fraction of CO in the product gas ranged below 0.2% for all experiments, it was neglected in the above calculation.

Dynamic Operation. Within this work, one dynamic load change was carried out. For this purpose, the plant was operated at 50% of the feed gas flow compared to the reference point from Table 2. During 30 s, the gas flow was ramped up to the reference point gas flow, while the inlet temperature of the heat transfer oil in the cooling coil of the reactor was held constant.

RESULTS AND DISCUSSION

General Remarks. The amount of water collected during catalyst activation in the first three runs was only between 75% (October 2019) and 88% (June 2020) of the amount indicated by the manufacturer's instructions for a fully activated catalyst, indicating that the catalyst was not activated completely. Only for the last run (August 2020), full catalyst activation was achieved by prolonging the catalyst activation period for several hours.

During the 100 h experimental runs at the methanation plant, a slight decrease in catalyst activity was observed. CO_2 conversion at the aforementioned reference point (process settings see Table 2) was between 79.0%...86.6% for all experiments. Besides a decreasing catalyst activity, possible reasons for these deviations are:

- Deviations in the stoichiometric number S (between 1.03 and 1.06, based on GC data)
- The catalyst amount used during the different experimental runs varied between 6.3 and 7.0 kg
- Degree of prerun catalyst activation in the external activation unit
- Measurement errors of the gas analytics

For all process conditions, a high product selectivity toward methane was found, with maximum concentrations of 0.2% for CO and 0.16% for C_2H_6 in the product gas. Mass balances for stationary operation added up better for hydrogen (96.0%...106.3%, mean value 101.5%) as compared to carbon (98.7%...118.3%, mean value 103.5%). An explanation for the high maximum value of the carbon balance may be the decomposition of the liquid phase at high stoichiometric numbers.

As only permanent gases were quantified by the GC, the amount of water in the hot product gas stream had to be calculated according to the reaction equation of CO_2 methanation.

Steady-State Operation. Figure 5 shows CO_2 conversion as a function of the reactor temperature. It has to be mentioned that in the P&I diagram in Figure 3, only one temperature measurement is shown for the sake of simplicity. In the actual setup a total of ten Pt100 thermometers are installed in the reactor, measuring the slurry phase temperature over the reactor length. Within the range of accuracy, all

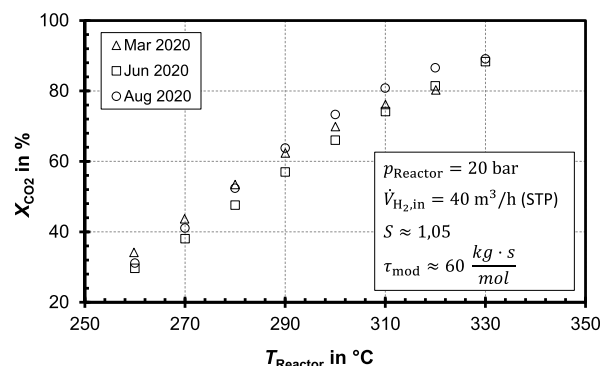


Figure 5. Temperature dependency of the CO_2 conversion.

thermometers showed the same temperature during steady-state operation, indicating an almost ideal isothermal behavior of the SBCR.

As expected, with a rising temperature, CO_2 conversion increases. Lefebvre et al.²⁵ observed a similar trend. The authors mention that rising temperatures accelerate reaction kinetics but also lead to a higher gas holdup and mass transfer in the SBCR due to a decreasing viscosity and surface tension of the liquid phase—all effects support a higher conversion rate.

Reaction kinetics has been described by Lefebvre et al.²⁶ based on the same three-phase system as used for the experiments described in this paper

$$r_{3\text{PM}} = 3.90699 \cdot 10^5 \cdot \exp\left(\frac{-79061}{R \cdot T}\right) \cdot \frac{c_{\text{H}_2,\text{L}}^{0.3} \cdot c_{\text{CO}_2,\text{L}}^{0.1}}{(1 + 1 \cdot c_{\text{H}_2\text{O},\text{L}})^{0.1}} \cdot K \quad (6)$$

Where R is the universal gas constant, T is the temperature at which the reaction takes place, $c_{i,\text{L}}$ is the concentration of the species i absorbed in the liquid phase, and K is a parameter expressing the reaction rate limitation due to approaching a chemical equilibrium (defined in ref 26).

Figure 6 shows that CO_2 conversion also increases with an increasing reactor pressure. Note that the doubling reactor

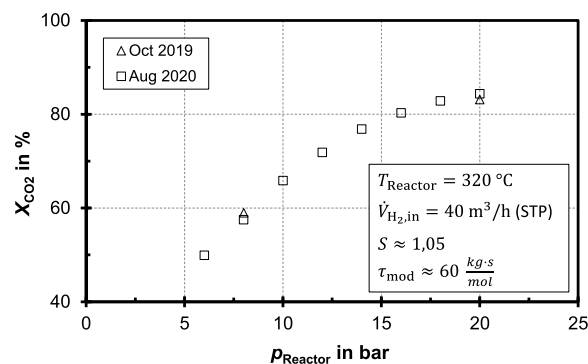


Figure 6. Pressure dependency of the CO_2 conversion.

pressure at a constant τ_{mod} means halving the superficial gas velocity: The superficial gas velocity is defined by

$$u_G = \frac{\dot{V}_G}{A_{\text{Reactor}}} \quad (7)$$

where \dot{V}_G is the reactant gas volume flow at a given temperature and pressure, and A_{Reactor} is the cross-sectional

area of the reactor. The reactor is operated at a constant input load of approximately 50 m³/h (STP) (see Table 2), resulting in superficial gas velocities from 0.029 m/s (20 bar) to 0.096 m/s (6 bar). As hydrodynamic data on, for example, the gas holdup are still not available, it is not possible to locate a shift between a homogeneous and heterogeneous flow regime. Such a shift may take place within the aforementioned range of u_G because the homogeneous regime has been found to extend to superficial gas velocities of 0.03–0.08 m/s.⁵¹ Therefore, at a nominal load ($u_G = 0.029$ m/s), the reactor is probably still operated in the homogeneous regime although solids often shift regime transition to lower superficial gas velocities.⁵² Generally, within the homogeneous regime, a higher reactant conversion than within the heterogeneous regime can be expected.⁴⁵ However, for more profound information, more experimental data is required on this specific system. This matter will be addressed in the ongoing research activities.

Lefebvre et al.²⁵ observed an increase in CO₂ conversion with an increasing pressure while keeping superficial gas velocity constant, that is, increasing the reactant load. The positive influence of pressure on CO₂ conversion can be explained by the equation for the mass transfer of a gas species i from the gas phase into the liquid phase as described in eq 8

$$\frac{\dot{N}_{i,G/L}}{V_L} = (k_L a)_i \cdot (c_{iL}^* - c_{iL}) \quad (8)$$

where $\dot{N}_{i,G/L}$ is the molar flow of the species i from the gas phase into the liquid phase, V_L is the volume of the liquid phase in the reactor, $(k_L a)_i$ is the volumetric mass transfer coefficient, c_{iL}^* is the equilibrium concentration of the species i at the interface, and c_{iL} is the concentration of the species i in the liquid bulk. Equation 8 holds for the simplifying assumptions that the liquid phase is completely back-mixed, c_{iL}^* is equal at every point in the reactor, and the relevant mass transfer resistance is only in the liquid boundary layer.

The solubility of the species i in the liquid phase at equilibrium can be expressed as

$$c_{iL}^* = \frac{p_i \cdot \rho_L}{H_i} \quad (9)$$

According to eq 8, mass transfer increases with an increasing c_{iL}^* . As liquid density and Henry's law constant H_i keep nearly constant, c_{iL}^* is directly proportional to the partial pressure of component i in the gas phase. If the mass transfer is significantly slower than the reaction rate at the catalyst surface, the liquid bulk concentration c_{iL} will be quite small. Thus, in an extreme case of c_{iL} being zero, the mass transfer is directly proportional to c_{iL}^* and therefore also to p_i for a constant $k_L a$.

A higher pressure has also been found to increase $k_L a$ because higher gas densities reduce the stable bubble size.^{53,54} As small bubbles have a higher surface-to-volume ratio and a slower rising velocity than large bubbles, $k_L a$ and gas holdup increase with pressure for a given superficial gas velocity.^{53,55} However, as indicated above, in the results presented here, the superficial gas velocity decreases with a rising pressure as the molar flow of reactants was kept constant, and therefore $(k_L a)_i$ is likely to decrease.

At 20 bar, the curve flattens though the equilibrium composition is not yet reached. Probably, at this point, the reaction kinetics at the catalyst surface begin to become the rate-determining step.

Figure 7 shows CO₂ conversion as a function of the stoichiometric number S of the feed gas. According to eq 3, a

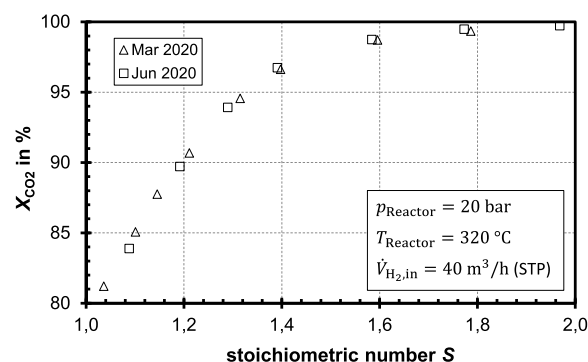


Figure 7. Influence of the stoichiometric number of the feed gas on the CO₂ conversion.

stoichiometric number of 1 represents a stoichiometric ratio of the reactants H₂ and CO₂ in the feed gas. With a stoichiometric number of 2, the feed gas contains twice the amount of H₂ stoichiometrically necessary for a complete CO₂ conversion. During the experiments discussed here, the H₂ flow was kept constant, and the CO₂ flow was varied in order to achieve S between 1 and 2.

In Figure 7, a steep increase in CO₂ conversion with increasing S is observed at near stoichiometric conditions, whereas for $S = 2$, nearly 100% of CO₂ conversion is achieved, which corresponds to the thermodynamic equilibrium under the given conditions. Evidently, H₂ conversion, which is not shown in Figure 7, decreases with an increasing S , resulting in a higher H₂ content of the product gas. Therefore, results at a high S may be less relevant for a technical application.

As the stoichiometric number was varied by variation of the CO₂ flow, keeping the H₂-flow constant, this means that with an increasing S , less CO₂ is fed to the reactor, and thus, τ_{mod} increases, which helps to understand the high degree of conversion achieved at higher values of S . Another influence may be an increasing reaction rate with an increasing H₂ concentration (see eq 6). For further clarification of these dependencies, future experiments will be carried out under a constant τ_{mod} .

Dynamic Operation. As mentioned in the introduction, the main advantage of the SBCR is the enhanced temperature control compared to other reactor concepts and, therefore, its robustness toward dynamic modes of operation. The dynamic behavior of the reactor with the three-phase system discussed here has already been investigated theoretically by Lefebvre^{28,37} using an axial dispersion model (ADM). Experimental data to prove the thermal robustness were still lacking because of the dominance of heat losses at the laboratory scale. Therefore, the dynamic operation of the pilot plant was of major interest.

First results on this matter are shown in Figure 8, where temperature and CO₂ conversion are plotted as a function of time for a gas load change from 20 to 40 m³/h (STP) of H₂. The CO₂ flow was adjusted simultaneously to keep a constant stoichiometric number of $S = 1.05$. To affect this load change, the gas input was ramped up within 30 s. The reactor temperature shows a very slow response to the gas load change, and the total increase in the reactor temperature is only about 14 K. In the present case, the temperature of the

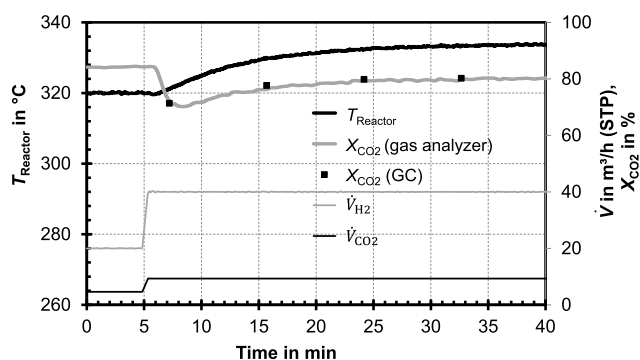


Figure 8. Reactor temperature and CO₂ conversion during a gas load change from 20 to 40 m³/h (STP) of H₂ ($p = 20$ bar, $S = 1.05$, a constant inlet temperature of the reactor cooling medium = 310 °C, data without dead time correction for concentration measurements).

cooling medium entering the cooling coil of the reactor was deliberately set to a constant value (310 °C) in order to observe the thermal response of the reactor under worst-case conditions. Evidently, in a real industrial application, the cooling medium temperature (or flow) would be adjusted by the process control system to the increasing heat production in order to achieve a constant reactor temperature. In any case, that should not be a challenging task considering the slow response time and the moderate increase in temperature shown in Figure 8.

The temperature curve from Figure 8 shows an asymptotic increase after the load change, as does the temperature curve of Lefebvre's reactor model for a load change from a 75 to 100% gas load (see refs 28 and 37). However, the model referred to a different reactor scale, input gas load, and reactor cooling parameters. To compare modeling data and plant data in detail, the model has to be adapted to the pilot plant in a future work package.

General Observations. In addition to the experimental data shown in this paper, a few general observations during the pilot plant operation are made:

- Reactions of the liquid phase (DBT): At the beginning of each run, an almost pure H₂ flow (95 vol % H₂ and 5 vol % N₂) was maintained for a few minutes before starting the methanation reaction by adding CO₂. During that process, up to 13 vol % of CH₄ was found in the product gas, while the product gas flow decreased to approximately one-fourth of the feed gas flow, and the reactor showed a considerable exothermal response. The abovementioned methane production without any CO₂ in the feed gas points toward the decomposition of DBT via hydrocracking. The exothermal response may be explained by the fact that DBT can be hydrogenated in the presence of catalysts to perhydrodibenzyltoluene (heat of hydrogenation -65.4 kJ/mol H₂⁵⁶), which is also investigated in the context of using DBT as a liquid organic hydrogen carrier (LOHC).^{57,58} While the aforementioned decomposition of DBT could represent a challenge for economic feasibility, hydrogenation of DBT is not expected to be a problem because of its reversibility. In situ dehydrogenation of the hydrogenated DBT might even provide additional H₂ for the methanation reaction. These questions, however, still need further systematic investigations.

- Condensate oil phase: A further issue is the evaporation of the liquid phase. Most of the liquid evaporated in the reactor is condensed in the first heat exchanger (HE101) and flows back directly to the reactor, while a smaller part remains in the vapor phase and is therefore condensed in the second heat exchanger (HE300) together with the reaction water formed by methanation. In order to keep the liquid level in the reactor constant, losses have to be replaced by adding fresh DBT with a dosing pump. The average volume fraction of the oil phase in the condensate is approximately 5%, as observed from the levels and phase boundary in the IBCs. The condensed oil has a lower density than water under ambient conditions, whereas DBT has a higher density than water, which may support the idea of the aforementioned hydrogenation reactions. In a large-scale application, the condensed oil phase may be re-fed into the reactor. These aspects, however, are still the subject of ongoing research activities.

CONCLUSIONS AND OUTLOOK

This work describes the setup and first experimental results from four campaigns on a 100 kW methanation pilot plant with an SBCR for catalytic CO₂ methanation. For a steady-state operation, the literature data from smaller laboratory plants confirm qualitatively the results from the significantly larger scale plant. As predicted, the CO₂ conversion rises with an increasing reactor pressure and also with an increasing stoichiometric number. Within the investigated process parameter settings, an increasing temperature also has a strong positive effect on CO₂ conversion. Therefore, not only the mass transfer but also reaction kinetics may be rate controlling. With regard to dynamic operation, the first experimental data in the 100 kW scale prove the thermal robustness of the SBCR methanation, previously predicted by Lefebvre's simulation work based on lab-scale experiments and the literature data.^{28,37} The experimental results indicate that hydrogenation of the heat transfer oil used as liquid phase—DBT—occurs during operation. Therefore, real liquid properties under reaction conditions may deviate from those of pure DBT. This effect is not described in the model up to now and is a part of ongoing research projects.

Future work will focus on the amplification of the data already acquired and on validation of the existing ADM from Lefebvre.^{28,37} Besides the reaction kinetics of the present system, which was described in ref 26, important parameters within the model are the gas holdup, volumetric mass transfer coefficients, and axial dispersion coefficients. These are calculated using correlations from the literature, which could lack the necessary accuracy. A significant step for in-depth validation of the model will be measuring the gas holdup in the SBCR as a part of future experimental work. Furthermore, hydrogenation of DBT has to be investigated in the context of changing liquid properties during methanation.

AUTHOR INFORMATION

Corresponding Author

Simon Sauersschell – Engler-Bunte-Institute—Division of Fuel Technology, Karlsruhe Institute of Technology, 76131 Karlsruhe, Germany; orcid.org/0000-0002-8877-8102; Email: simon.sauerschell@kit.edu

Authors

Siegfried Bajohr – Engler-Bunte-Institute—Division of Fuel Technology, Karlsruhe Institute of Technology, 76131 Karlsruhe, Germany

Thomas Kolb – Engler-Bunte-Institute—Division of Fuel Technology, Karlsruhe Institute of Technology, 76131 Karlsruhe, Germany; DVGW Research Center at Engler-Bunte-Institute of Karlsruhe Institute of Technology, 76131 Karlsruhe, Germany

Complete contact information is available at:

<https://pubs.acs.org/10.1021/acs.energyfuels.2c00655>

Notes

The authors declare no competing financial interest.

ACKNOWLEDGMENTS

The construction of the methanation plant as a part of the Energy Lab 2.0 was funded by the state of Baden-Württemberg, the Federal Ministry of Education and Research (BMBF), and the Federal Ministry for Economic Affairs and Energy (BMWi). Plant operation and further research have received financial support from the first phase of the Kopernikus P2X project (funded by the BMBF) and the ongoing research projects MethQuest and RegEnZell (both funded by the BMWi) and SEKO (funded by the BMBF). The authors also express their thanks to the operating team (head: Raphael Küchlin) for making continuous plant operation possible.

SYMBOLS USED

A_{Reactor} = cross-sectional area of the reactor
 a = gas–liquid interfacial area referred to the liquid volume, 1/m
 c = concentration, mol/m³
 c_{iL} = concentration of species i in the liquid phase, mol/m³
 c_{iL}^* = gas solubility at equilibrium, mol/m³
 d_{Reactor} = inner reactor diameter, mm
 H = Henry's law constant, bar kg/mol
 K = parameter to express the reaction rate limitation due to approaching the chemical equilibrium. Defined in ref 26
 k_L = liquid-side mass transfer coefficient, m/s
 $k_L a$ = volumetric mass transfer coefficient (product of k_L and a), 1/s
 M = molecular mass, g/mol
 m = mass, kg
 \dot{N} = molar flow, mol/s
 p = pressure (absolute), bar
 R = universal gas constant, J/(mol K)
 r_{3PM} = reaction rate for three-phase methanation, mol/(s kg)
 S = stoichiometric number
 T = temperature, °C
 u = velocity, m/s
 V = volume, m³
 \dot{V} = volume flow, m³/h
 X = conversion
 x_{50} = particle size at the 50% point of the cumulative size distribution, μm
 y = mole fraction
 $\Delta_R H^0$ = standard enthalpy of reaction, kJ/mol

GREEK LETTERS

ρ = density, kg/m³

ν = kinematic viscosity, mm²/s
 ν = stoichiometric coefficient
 τ_{mod} = modified residence time, kg s/mol

SUB- AND SUPERSCRIPTS

cat = catalyst
 G = gas
 i = species i
 in = input
 L = liquid
 max = maximum
 out = output
 vap = vapor

ABBREVIATIONS

DBT = dibenzyltoluene
 EBI = Engler-Bunte-Institut
 GC = gas chromatograph
 KIT = Karlsruhe Institute of Technology
 LOHC = liquid organic hydrogen carrier
 NDIR = nondispersive infrared (sensor)
 STP = standard temperature and pressure (0 °C; 1.013 bar)
 PEM = proton exchange membrane
 P&ID = piping and instrumentation diagram
 PtG = power-to-gas
 SBCR = slurry bubble column reactor
 SNG = synthetic natural gas
 TCD = thermal conductivity detector

REFERENCES

- (1) United Nations Framework Convention on Climate Change, Paris Agreement—Status of Ratification. <https://unfccc.int/process/the-paris-agreement/status-of-ratification> (accessed Feb 1, 2022).
- (2) Sterner, M.; Stadler, M. *Handbook of Energy Storage: Demand, Technologies, Integration*; Springer Berlin: Berlin, s.l., 2018.
- (3) Store &Go website. <https://www.storeandgo.info> (accessed April 27, 2022).
- (4) Schollenberger, D.; Bajohr, S.; Gruber, M.; Reimert, R.; Kolb, T. Scale-Up of Innovative Honeycomb Reactors for Power-to-Gas Applications – The Project Store&Go. *Chem. Ing. Tech.* **2018**, *90*, 696–702.
- (5) Adolf, J.; Balzer, C.; Kofod, M.; Lenz, B.; Lischke, A.; Knitschky, G.; Witz, F.; Wendland, M. Shell LNG-Study: Liquefied Natural Gas—New Energy for Ships and Trucks?. 2019 https://www.shell.de/about-us/newsroom/shell-lng-study/_jcr_content/root/main/containersection-0/simple/call_to_action/links/item1.stream/0/8c14ea6b6b92b887fba9026055a12cd0e9b817779cec881fdf3910537b5db666/lng-study-uk-einzelseiten.pdf (accessed April 30, 2022).
- (6) Thunman, H.; Seemann, M.; Berdugo Vilches, T.; Maric, J.; Pallares, D.; Ström, H.; Berndes, G.; Knutsson, P.; Larsson, A.; Breitholtz, C.; Santos, O. Advanced biofuel production via gasification - lessons learned from 200 man-years of research activity with Chalmers' research gasifier and the GoBiGas demonstration plant. *Energy Sci. Eng.* **2018**, *6*, 6–34.
- (7) Bains, P.; Psarras, P.; Wilcox, J. CO₂ capture from the industry sector. *Prog. Energy Combust. Sci.* **2017**, *63*, 146–172.
- (8) McQueen, N.; Gomes, K. V.; McCormick, C.; Blumanthal, K.; Pisciotta, M.; Wilcox, J. A review of direct air capture (DAC): Scaling up commercial technologies and innovating for the future. *Prog. Energy* **2021**, *3*, 032001.
- (9) Kopyscinski, J.; Schildhauer, T. J.; Biollaz, S. M. A. Production of synthetic natural gas (SNG) from coal and dry biomass – A technology review from 1950 to 2009. *Fuel* **2010**, *89*, 1763–1783.

- (10) Rönsch, S.; Schneider, J.; Matthischke, S.; Schlüter, M.; Götz, M.; Lefebvre, J.; Prabhakaran, P.; Bajohr, S. Review on methanation – From fundamentals to current projects. *Fuel* **2016**, *166*, 276–296.
- (11) Hiller, H.; Reimert, R.; Stöner, H.-M. Gas Production, 1. Introduction. *Ullmann's Encyclopedia of Industrial Chemistry*; Wiley: Chichester, 2010.
- (12) Appl, M. Ammonia, 2. Production Processes. *Ullmann's Encyclopedia of Industrial Chemistry*; Wiley: Chichester, 2010.
- (13) Panek, J. M.; Grasser, J. *Practical Experience Gained During the First Twenty Years of Operation of the Great Plains Gasification Plant and Implications for Future Projects*, 2006.
- (14) Xu, J.; Yang, Y.; Li, Y.-W. Recent development in converting coal to clean fuels in China. *Fuel* **2015**, *152*, 122–130.
- (15) Mills, S. J. *Low Quality Coals - Key Commercial, Environmental and Plant Considerations*; IEA Clean Coal Centre: London, 2016.
- (16) van der Zwaan, B.; Detz, R.; Meulendijks, N.; Buskens, P. Renewable natural gas as climate-neutral energy carrier? *Fuel* **2022**, *311*, 122547.
- (17) Bailera, M.; Lisbona, P.; Romeo, L. M.; Espatolero, S. Power to Gas projects review: Lab, pilot and demo plants for storing renewable energy and CO₂. *Renewable Sustainable Energy Rev.* **2017**, *69*, 292–312.
- (18) Specht, M.; Brellocks, J.; Frick, V.; Stürmer, B.; Zuberbühler, U. 4.4.3.1 Technical Realization of Power-to-Gas Technology (P2G®): Production of Substitute Natural Gas by Catalytic Methanation of H₂/CO₂. In *Natural Gas and Renewable Methane for Powertrains: Future Strategies for a Climate-Neutral Mobility*, 1st ed.; van Basshuysen, R. Ed.; Springer-Verlag, s.l., 2016; pp 141–167.
- (19) Schlautmann, R.; Böhm, H.; Zauner, A.; Mörs, F.; Tichler, R.; Graf, F.; Kolb, T. Renewable Power-to-Gas: A Technical and Economic Evaluation of Three Demo Sites Within the STORE&GO Project. *Chem. Ing. Tech.* **2021**, *93*, 568–579.
- (20) Farsi, S.; Liang, S.; Pfeifer, P.; Dittmeyer, R. Application of evaporation cooling in a microstructured packed bed reactor for decentralized CO₂ methanation. *Int. J. Hydrogen Energy* **2021**, *46*, 19971–19987.
- (21) Guilera, J.; Boeltken, T.; Timm, F.; Mallol, I.; Alarcón, A.; Andreu, T. Pushing the Limits of SNG Process Intensification: High GHSV Operation at Pilot Scale. *ACS Sustainable Chem. Eng.* **2020**, *8*, 8409–8418.
- (22) Huynh, H. L.; Yu, Z. CO₂ Methanation on Hydrotalcite-Derived Catalysts and Structured Reactors: A Review. *Energy Technol.* **2020**, *8*, 1901475.
- (23) Baena-Moreno, F. M.; González-Castaño, M.; Navarro de Miguel, J. C.; Miah, K. U. M.; Ossenbrink, R.; Odriozola, J. A.; Arellano-García, H. Stepping toward Efficient Microreactors for CO₂ Methanation: 3D-Printed Gyroid Geometry. *ACS Sustainable Chem. Eng.* **2021**, *9*, 8198–8206.
- (24) Biegger, P.; Kirchbacher, F.; Medved, A.; Miltner, M.; Lehner, M.; Harasek, M. Development of Honeycomb Methanation Catalyst and Its Application in Power to Gas Systems. *Energies* **2018**, *11*, 1679.
- (25) Lefebvre, J.; Götz, M.; Bajohr, S.; Reimert, R.; Kolb, T. Improvement of three-phase methanation reactor performance for steady-state and transient operation. *Fuel Process. Technol.* **2015**, *132*, 83–90.
- (26) Lefebvre, J.; Trudel, N.; Bajohr, S.; Kolb, T. A study on three-phase CO₂ methanation reaction kinetics in a continuous stirred-tank slurry reactor. *Fuel* **2018**, *217*, 151–159.
- (27) Lefebvre, J.; Bajohr, S.; Kolb, T. A comparison of two-phase and three-phase CO₂ methanation reaction kinetics. *Fuel* **2019**, *239*, 896–904.
- (28) Lefebvre, J.; Bajohr, S.; Kolb, T. Modeling of the transient behavior of a slurry bubble column reactor for CO₂ methanation, and comparison with a tube bundle reactor. *Renewable Energy* **2020**, *151*, 118–136.
- (29) Hammer, H. *Zur Reaktionstechnik von Blasensäulen-Reaktoren mit suspendierten Katalysator. Habilitationsschrift*; Technische Universität Berlin, 1968.
- (30) Alpert, S. B.; Sherwin, B. M.; Cochran, N. P. Slurry Phase Methanation Process. U.S. Patent 3,989,734 A, 1976.
- (31) Blum, D. B.; Sherwin, M. B.; Frank, M. E. *Liquid Phase Methanation of High Concentration CO Synthesis Gas, Methanation of Synthesis Gas*; American Chemical Society, 1974; pp 44–56.
- (32) Chem Systems Inc. *Liquid Phase Methanation Pilot Plant Installation and Operation: Interim Annual Report*, July 1, 1967–June 30, 1977.
- (33) U.S. Department of Energy, *Coal Conversion*. 1978 technical report, 1979.
- (34) Götz, M.; Ortloff, F.; Reimert, R.; Basha, O.; Morsi, B. I.; Kolb, T. Evaluation of Organic and Ionic Liquids for Three-Phase Methanation and Biogas Purification Processes. *Energy Fuels* **2013**, *27*, 4705–4716.
- (35) Götz, M.; Reimert, R.; Bajohr, S.; Schnetzer, H.; Wimberg, J.; Schubert, T. J. S.; Thomas, J. S. Long-term thermal stability of selected ionic liquids in nitrogen and hydrogen atmosphere. *Thermochim. Acta* **2015**, *600*, 82–88.
- (36) Götz, M. *Methanisierung im Dreiphasen-Reaktor*. Dissertation. Karlsruher Institut für Technologie (KIT), 2014.
- (37) Lefebvre, J. *Three-phase CO₂ Methanation – Methanation Reaction Kinetics and Transient Behavior of a Slurry Bubble Column Reactor*; Dr. Hut: München, 2019.
- (38) Götz, M.; Lefebvre, J.; Mörs, F.; Reimert, R.; Graf, F.; Kolb, T. Hydrodynamics of organic and ionic liquids in a slurry bubble column reactor operated at elevated temperatures. *Chem. Eng. J.* **2016**, *286*, 348–360.
- (39) Zhang, J.; Bai, Y.; Zhang, Q.; Wang, X.; Zhang, T.; Tan, Y.; Han, Y. Low-temperature methanation of syngas in slurry phase over Zr-doped Ni/γ-Al₂O₃ catalysts prepared using different methods. *Fuel* **2014**, *132*, 211–218.
- (40) Meng, F.; Li, Z.; Liu, J.; Cui, X.; Zheng, H. Effect of promoter Ce on the structure and catalytic performance of Ni/Al₂O₃ catalyst for CO methanation in slurry-bed reactor. *J. Nat. Gas Sci. Eng.* **2015**, *23*, 250–258.
- (41) Meng, F.; Li, X.; Li, M.; Cui, X.; Li, Z. Catalytic performance of CO methanation over La-promoted Ni/Al₂O₃ catalyst in a slurry-bed reactor. *Chem. Eng. J.* **2017**, *313*, 1548–1555.
- (42) Yoshida, F.; Akita, K. Performance of gas bubble columns: Volumetric liquid-phase mass transfer coefficient and gas holdup. *AIChE J.* **1965**, *11*, 9–13.
- (43) van Dierendonck, L. L. *Vergrotingsregels voor Gasbelwassers*. Ph.D. Thesis, University of Twente, The Netherlands, 1970.
- (44) Forret, A.; Schweitzer, J. M.; Gauthier, T.; Krishna, R.; Schweich, D. Scale Up of Slurry Bubble Reactors. *Oil Gas Sci. Technol.* **2006**, *61*, 443–458.
- (45) Deckwer, W.-D. *Reaktionstechnik in Blasensäulen*; Otto Salle Verlag, 1985.
- (46) Rollbusch, P.; Bothe, M.; Becker, M.; Ludwig, M.; Grünewald, M.; Schlüter, M.; Franke, R. Bubble columns operated under industrially relevant conditions – Current understanding of design parameters. *Chem. Eng. Sci.* **2015**, *126*, 660–678.
- (47) Karlsruher Institut für Technologie (KIT), Energy Lab 2.0: The Future Energy System in the Focus. https://www.elab2.kit.edu/downloads/Broschüre_EL2_2018.pdf (accessed April 8, 2020).
- (48) Held, M.; Schollenberger, D.; Sauerschell, S.; Bajohr, S.; Kolb, T. Power-to-Gas: CO₂ Methanation Concepts for SNG Production at the Engler-Bunte-Institut. *Chem. Ing. Tech.* **2020**, *92*, 595–602.
- (49) Dahmen, N.; Abeln, J.; Eberhard, M.; Kolb, T.; Leibold, H.; Sauer, J.; Stapf, D.; Zimmerlin, B. The bioliq process for producing synthetic transportation fuels. *WIREs Energy Environ.* **2017**, *6*, No. e236.
- (50) Sasol GmbH. Product information: Marlotherm® SH http://www.sasolgermany.de/fileadmin/images/marlotherm/MARLOTHERM_SH_info_e.pdf (accessed April 9, 2020).
- (51) Deen, N. G.; Mudde, R. F.; Kuipers, J. A. M.; Zehner, P.; Kraume, M. Bubble Columns. *Ullmann's Encyclopedia of Industrial Chemistry*; Wiley, 2010.

(52) Mörs, F.; Graf, F.; Kolb, T. Reaktoren für Dreiphasen-Reaktionen: Suspensionsreaktoren. In *Handbuch Chemische Reaktoren: Grundlagen und Anwendungen der Chemischen Reaktionstechnik*; Reschetilowski, W., Ed.; Springer Berlin Heidelberg: Berlin, Heidelberg, 2019; pp 1–32.

(53) Lin, T.-J.; Tsuchiya, K.; Fan, L.-S. Bubble flow characteristics in bubble columns at elevated pressure and temperature. *AIChE J.* **1998**, *44*, 545–560.

(54) Wilkinson, P. M.; Dierendonck, L. L. v. Pressure and gas density effects on bubble break-up and gas hold-up in bubble columns. *Chem. Eng. Sci.* **1990**, *45*, 2309–2315.

(55) Jordan, U.; Schumpe, A.; Terasaka, K.; Kundu, G. Stoffübergang in Druckblasensäulen mit organischen Flüssigkeiten. *Chem. Ing. Tech.* **2001**, *73*, 982–985.

(56) Müller, K.; Stark, K.; Emel'yanenko, V. N.; Varfolomeev, M. A.; Zaitsau, D. H.; Shoifet, E.; Schick, C.; Verevkin, S. P.; Arlt, W. Liquid Organic Hydrogen Carriers: Thermophysical and Thermochemical Studies of Benzyl- and Dibenzyl-toluene Derivatives. *Ind. Eng. Chem. Res.* **2015**, *54*, 7967–7976.

(57) Preuster, P.; Papp, C.; Wasserscheid, P. Liquid Organic Hydrogen Carriers (LOHCs): Toward a Hydrogen-free Hydrogen Economy. *Acc. Chem. Res.* **2017**, *50*, 74–85.

(58) Jorschick, H.; Preuster, P.; Dürr, S.; Seidel, A.; Müller, K.; Bösmann, A.; Wasserscheid, P. Hydrogen storage using a hot pressure swing reactor. *Energy Environ. Sci.* **2017**, *10*, 1652–1659.

Recommended by ACS

Biogas to Syngas through the Combined Steam/Dry Reforming Process: An Environmental Impact Assessment

Nicola Schiaroli, Carlo Lucarelli, *et al.*

FEBRUARY 18, 2021
ENERGY & FUELS

READ 

Utilization of Water Utility Lime Sludge for Flue Gas Desulfurization in Coal-Fired Power Plants: Part III. Testing at a Higher Scale and Assessment of Selected...

Seyed A. Dastgheib, Craig Patterson, *et al.*

OCTOBER 29, 2019
ENERGY & FUELS

READ 

Assessment of Concentration and Temperature Distribution in a Berty Reactor for an Exothermic Reaction

Scott D. Anderson, Gregor D. Wehinger, *et al.*

JULY 12, 2022
INDUSTRIAL & ENGINEERING CHEMISTRY RESEARCH

READ 

Modeling Carbon-to-Nitrogen Ratio Influence on Biogas Production by the 4th-order Runge–Kutta Method

Latif Fagbemi, Evrard Karol Ekouedjen, *et al.*

AUGUST 16, 2019
ENERGY & FUELS

READ 

Get More Suggestions >